ACE2 inhibition worsens glomerular injury in association with increased ACE expression in streptozotocin-induced diabetic mice

MJ Soler[1], J Wysocki[1], M Ye[1], J Lloveras[2], Y Kanwar[3] and D Batlle[1]

[1]Division of Nephrology and Hypertension, Department of Medicine, The Feinberg School of Medicine, Northwestern University, Chicago, Illinois, USA; [2]Department of Nephrology, Hospital del Mar, Universitat Autònoma de Barcelona, Barcelona, Spain and [3]Department of Pathology, Feinberg School of Medicine, Northwestern University, Chicago, Illinois, USA

Angiotensin converting enzyme 2 (ACE2) is localized to the glomerular epithelial cells. Since ACE2 promotes the degradation of angiotensin II, a decrease in ACE2 activity could lead to the development of glomerular injury. We gave a specific ACE2 inhibitor, MLN-4760, for 4 weeks to mice rendered diabetic with streptozotocin. The urinary albumin/creatinine ratio was increased along with expansion of the glomerular matrix in diabetic mice treated with the inhibitor compared to the vehicle-treated mice. Glomerular staining of ACE was increased in the diabetic group and was further significantly increased in the diabetic group treated with MLN-4760. In renal vessels, ACE expression was also increased in the diabetic mice and, again, further increased in those diabetic mice treated with the ACE2 inhibitor. Our study shows that chronic pharmacologic ACE2 inhibition worsens glomerular injury in streptozotocin-induced diabetic mice in association with increased ACE expression.

Kidney International (2007) **72,** 614–623; doi:10.1038/sj.ki.5002373; published online 20 June 2007

KEYWORDS: ACE; ACE2; diabetic nephropathy; renal histology; albuminuria; ACE2 inhibition

Correspondence: *D Batlle, Division of Nephrology and Hypertension, Department of Medicine, The Feinberg School of Medicine, Northwestern University, Chicago, Illinois 60611, USA. E-mail: d-batlle@northwestern.edu*

Received 21 November 2006; revised 12 April 2007; accepted 1 May 2007; published online 20 June 2007

Angiotensin converting enzyme (ACE), a dipeptidyl carboxypeptidase, is a key enzyme of the renin angiotensin system (RAS) that converts angiotensin (Ang) I to II.[1] (ACE)-2 is a homologue of ACE, which shares 42% sequence identity to the N- and C-terminal domains of somatic ACE.[1–3] ACE2 cleaves Ang II into Ang 1-7 and degrades Ang I to Ang 1-9.[2,4,5] We first advanced the notion that ACE2 could be renoprotective in diabetic mice, particularly in combination with reduced ACE activity.[6] In support of this concept, we have shown that the pharmacological inhibition of ACE2 worsens albuminuria in the *db/db* model of diabetes.[7] The importance of this enzyme is also apparent from recent studies with the ACE2 knockout showing that male, but not female, mice developed renal pathological lesions.[8] Other studies in ACE2 knockout have suggested an important role of this enzyme in protecting against lung injury[9] and an exaggerated blood pressure increase after Ang II infusion.[10]

Because the RAS plays a key role in renal injury,[11–13] there is increasing interest in examining ACE2 expression in the kidney, particularly in diabetic nephropathy.[6,7,14] We have shown recently that in the kidney, ACE and ACE2 are localized within distinct glomerular structures.[7] ACE2 was expressed mainly in visceral epithelial cells (podocytes), and in parietal epithelial cells of the Bowman's capsule. Moreover, we found that ACE2 protein expression in glomeruli from *db/db* mice was decreased, whereas ACE protein expression, by contrast, was increased.[7] It should be noted that in the *db/db* mice, the pattern of tubular expression of ACE and ACE2 (i.e., low ACE and high ACE2) is just the opposite than that seen in glomeruli.[6,15] In the present study, we investigated the effect of chronic pharmacological ACE2 inhibition in the streptozotocin (STZ) model of diabetes in terms of (1) histological damage, (2) albumin excretion rates, and (3) ACE expression.

RESULTS

General findings

Eight weeks after STZ administration, blood glucose was increased as compared to control mice of similar age (19 weeks of age) (Table 1). In STZ-treated mice given

MLN-4760, glucose levels were not significantly different from STZ-treated mice given vehicle (Table 1). An increase in both, right and left kidney weight was observed in STZ-treated mice as compared to non-diabetic controls. STZ-treated mice given MLN-4760 had a modest but significant decrease in body weight, but a significant increase in kidney weight as compared to STZ mice given vehicle (Table 1). Therefore, the ratio of kidney/body weight was increased in STZ-treated mice and further increased in STZ-treated mice given MLN-4760 (Table 1).

There were significant differences in urinary albumin excretion between the three groups studied (Figure 1). In STZ mice treated with vehicle, urinary albumin excretion was approximately 10-fold higher than in vehicle treated non-diabetic controls (237 ± 88 vs 22 ± 5 μg/mg, respectively, $P < 0.05$) (Table 1). After 4 weeks of MLN-4760 administration to STZ-treated mice, urinary albumin excretion was significantly higher than in STZ mice treated with vehicle (1107 ± 251 vs 237 ± 88 μg/mg, respectively, $P < 0.05$) (Figure 1).

Table 1 | Effect of MLN-4760 on STZ-treated mice

	Control+vehicle	STZ+vehicle	STZ+MLN-4760
n	5	10	14
Blood glucose (mg/dl)	154.6 ± 8.4	438.2 ± 49.1*	$501.1 \pm 39.3^{\dagger}$
Body weight (g)	21.8 ± 0.4	20.0 ± 0.6*	$18.3 \pm 0.4^{\dagger,\ddagger}$
Right kidney weight (mg)	137.8 ± 5.4	180.9 ± 8.0*	$217.6 \pm 10.6^{\dagger,\ddagger}$
Ratio kidneys/body weight	0.012 ± 0.0004	0.018 ± 0.001*	$0.023 \pm 0.001^{\dagger,\ddagger}$
Albuminuria/creatinine (μg/mg)	21.6 ± 5.3	236.7 ± 88.0*	$1107.4 \pm 250.9^{\dagger,\ddagger}$

Control+vehicle (n=5): non-diabetic control mice given vehicle; STZ+vehicle (n=10): streptozotocin-induced diabetic mice given vehicle; STZ+MLN-4760 (n=14): STZ mice given MLN-4760.
Data are expressed as means $\pm$ s.e.
*$P < 0.05$ control+vehicle vs STZ+vehicle.
$^{\dagger}P \leqslant 0.001$ control+vehicle vs STZ+MLN-4760.
$^{\ddagger}P \leqslant 0.05$ STZ+vehicle vs STZ+MLN-4760. Mann–Whitney test.

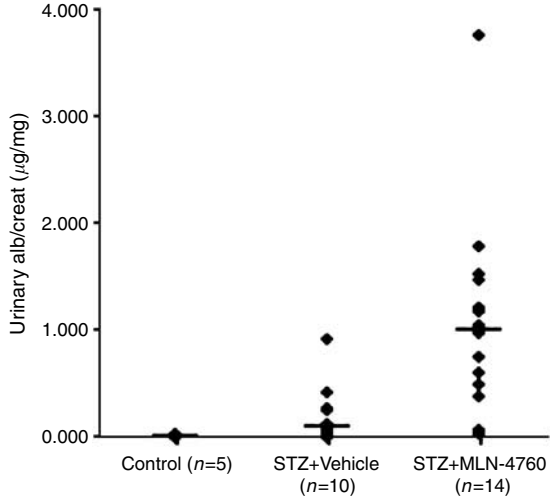

Figure 1 | Urinary albumin/creatinine ratio after 4 weeks of MLN-4760 or vehicle administration. Each point reflects data from one animal in each group. The mean $\pm$ s.e. of the three groups is significantly different ($P < 0.05$).

ACE2 activity and mRNA expression

ACE2 activity was measured in kidney cortex from STZ mice treated with MLN-4760 and the vehicle-treated STZ counterparts. ACE2 activity in kidney cortex from STZ mice given MLN-4760 for 4 weeks was decreased as compared to vehicle-treated animals also given STZ (1.13 ± 0.15 RFU (relative fluorescence units)/μg protein/h vs 12.3 ± 1.6, respectively, $P < 0.001$). This represents a 90% inhibition by MLN-4760 as compared to STZ mice given vehicle. ACE2 mRNA was decreased in kidney cortex from STZ mice given MLN-4760, as compared to STZ mice given vehicle also for 4 weeks (0.63 ± 0.08 vs 1.10 ± 0.24, respectively, $P < 0.05$).

MLN-4760 specificity

MLN-4760 has been shown to specifically inhibit ACE2 activity of purified human recombinant ACE2 protein.[15] We wanted to test the specificity of this compound for murine ACE2 protein.

We tested the inhibitory effect of MLN-4760 on mouse recombinant (mr)ACE2 (20 nM; R&D Systems, Minneapolis, MN, USA) at concentrations ranging from 100 pM to 100 μM (Figure 2a). MLN-4760 quenched the fluorescence signal completely at 1 μM (Figure 2a). The ACE inhibitor, captopril, by contrast, failed to quench fluorescence when incubated with mrACE2 at a concentration up to 100 μM (Figure 2a).

MLN-4760 specificity was also shown in isolated mouse glomeruli and renal cortex. MLN-4760 (1 μM) did not inhibit ACE activity either in glomerular isolates or in renal cortex (Figure 2b and c), whereas captopril at the same concentration reduced it to $35.3\% \pm 17.6$ and $8.4\% \pm 1.9$ of control, respectively.

Effect of MLN-4760 on plasma levels of Ang II

There was no significant difference in the plasma levels of Ang II between control and STZ mice (36.1 ± 16.5 vs 45.4 ± 12.2 fmol/ml, respectively, $P = 0.62$). Moreover, plasma Ang II levels in STZ mice given MLN-4760 were not significantly different as compared to STZ mice treated with vehicle (37.4 ± 10.4 vs 45.4 ± 12.2 fmol/ml, respectively, $P = 0.66$).

Renal histological findings

The light microscopy findings in kidneys from control, vehicle-treated STZ mice, and MLN-4760-treated STZ mice are summarized in Table 2. Glomerular mesangial matrix was increased in STZ-treated mice as compared to non-diabetic controls (Figure 3b and a, respectively), and further increased in STZ mice receiving MLN-4760 (Figure 3c). A semiquantitative analysis revealed a significant increase in MLN-4760-treated STZ mice as compared to STZ mice treated with vehicle (Table 2). Using computer-linked image analysis, the glomerular tuft area was increased in both STZ-treated groups compared to the non-diabetic control group (Table 2).

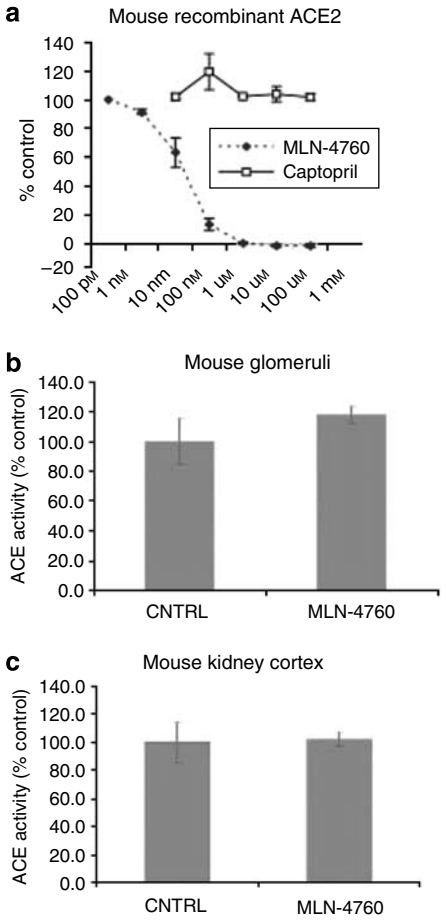

Figure 2 | (**a**) The effect of MLN-4760 on murine recombinant ACE2 (20 nM) was assessed using fluorgenic substrate 7-methoxycoumarin-Tyr-Val-Ala-Asp-Ala-Pro-Lys (2,4-dinitrophenyl). Fluorescence under control conditions (100%, addition of buffer) and after addition of a specific ACE2 inhibitor, MLN-4760, or ACE inhibitor captopril at concentrations ranging from 100 pM to 100 μM). Each data point represent mean $\pm$ s.e. calculated from duplicate wells and is expressed as percent of to the values obtained in control experiments (buffer control measured in quintuplicate wells). The lack of inhibition of MLN-4760 on tissue ACE activity is shown in (**b**) (glomerular isolates) and (**c**) (renal cortex). Protein lysates from isolated glomeruli or kidney cortex were incubated without (buffer control) or with addition of MLN-4760 (1 μM). Glomeruli were pooled from four mice. The values represent means of triplicate wells and were set to 100% (buffer control).

There was no significant difference in glomerular size between the STZ-treated mice receiving vehicle or MLN-4760 (Table 2). Glomerular cellularity was increased in STZ mice treated with vehicle as compared to the non-diabetic control group (Figure 2b and a, respectively). MLN-4760-treated STZ mice, however, had decreased glomerular cellularity as compared to vehicle-treated STZ mice (Table 2).

In renal arterioles from STZ mice, the tunica media layer showed increased thickness as compared to non-diabetic controls, and in MLN-4760-treated STZ mice, vascular thickness increased as compared to vehicle-treated STZ mice (Table 2).

In vehicle- and MLN-4760-treated STZ mice, light photomicrographs of kidney sections revealed atrophy of medulla (Figure 4). Atrophy of the medulla and its tubules was most notable in MLN-4760-treated STZ mice. By contrast, tubular hypertrophy was observed in the cortical area (Figure 4), as reported previously in STZ-induced diabetic rats.[16] Tubular enlargement was seen in both STZ groups, but tubules with enlarged nuclei were readily seen in the MLN-4760-treated group, suggesting accentuated hypertrophic response in this group. That MLN-4760-treated mice had tubular hypertrophy can also be inferred from the increased kidney weight and kidney/body weight ratio in MLN-4760-treated STZ mice as compared to vehicle treated-STZ mice (Table 1).

In the tubulointerstitial area, fibronectin and collagen I staining were increased significantly in STZ-treated mice as compared to the non-diabetic control group (Table 2). In MLN-4760-treated STZ mice, fibronectin and collagen I expression were increased as compared to STZ mice treated with vehicle, but the difference did not reach statistical significance (Table 2). The two markers of fibrosis were further quantified at the mRNA level. Concordant with the immunostaining findings, fibronectin mRNA was increased in kidney cortex from STZ mice treated with vehicle as compared to non-diabetic controls (12.81 ± 2.58 vs 1.13 ± 0.06 respectively, $P = 0.001$). There was no significant difference in fibronectin mRNA in renal cortex between the STZ mice receiving vehicle and MLN-4760 treated animals (12.81 ± 2.58 vs 15.50 ± 1.91 respectively, $P = 0.41$). Likewise,

Table 2 | Light microscopy findings

	Control+vehicle	STZ+vehicle	STZ+MLN-4760
Mesangial matrix expansion	1.00 ± 0.00	2.50 ± 0.22*	$3.86 \pm 0.10^{\#,\$}$
Glomerular tuft area (μm^2)	2350.4 ± 97.8	3071.2 ± 87.2*	$3204.1 \pm 67.9^{\#}$
Glomerular cellularity (cells/gcs)	29.4 ± 2.2	39.6 ± 0.82*	$34.13 \pm 0.73^{\#,\$}$
Vascular thickness	1.00 ± 0.00	1.55 ± 0.24*	$3.19 \pm 0.26^{\#,\$}$
Inmunohistochemistry (tubulointerstitial area)			
Fibronectin	1.45 ± 0.06	2.06 ± 0.25*	$2.40 \pm 0.12^{\#}$
Collagen I	0.37 ± 0.06	1.54 ± 0.27*	$2.16 \pm 0.16^{\#}$

H&E, hematoxylin and eosin stain; PAS, periodic acid-Schiff.
Data are expressed as means $\pm$ s.e. *$P < 0.05$ control+vehicle vs STZ+vehicle. $^{\#}P \leqslant 0.05$ control+vehicle vs STZ+MLN-4760. $^{\$}P \leqslant 0.05$ STZ+vehicle vs STZ+MLN-4760. Mann–Whitney test.
Optical histology: mesangial matrix expansion, glomerular hypercellularity, glomerular hypertrophy, and vascular thickness were evaluated on H&E stain and PAS sections by a nephropathologist.

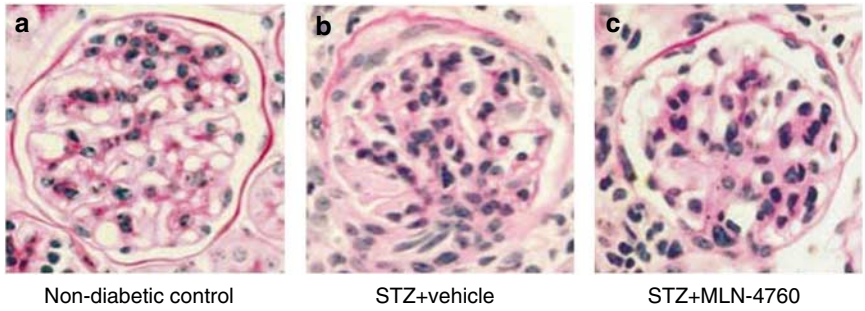

Figure 3 | (**a**) Kidney sections from non-diabetic, (**b**) STZ-treated mice given vehicle, and (**c**) STZ-treated mice receiving MLN-4760. Periodic acid-Schiff staining in glomerulus (original magnification ×600): (**b**) STZ-treated mice given vehicle show mild mesangial expansion and hypercellularity as compared with (**a**) non-diabetic mice. (**c**) STZ-treated mice given MLN-4760 show increased mesangial expansion as compared to STZ-treated mice given (**b**) vehicle.

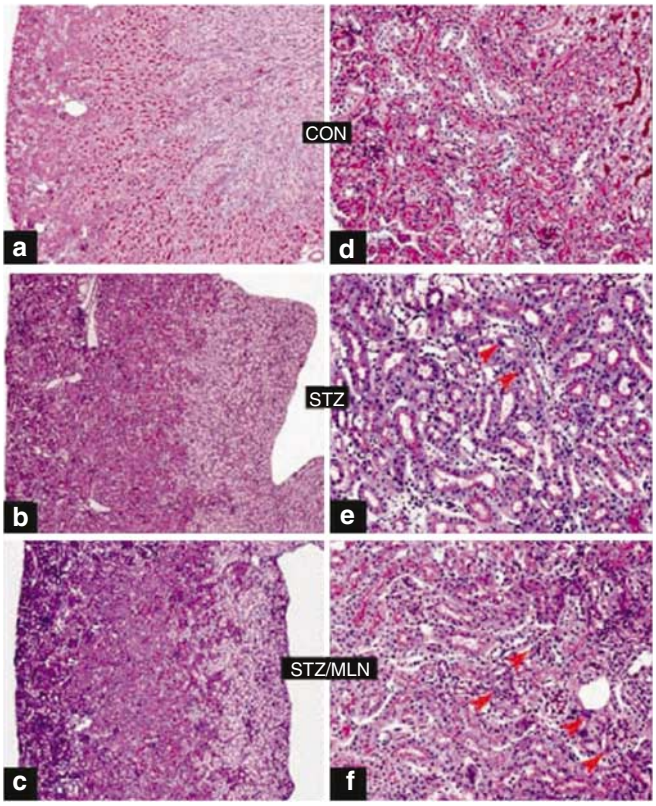

Figure 4 | Light photomicrographs of kidney sections from (**a** and **d**) non-diabetic controls, (**b** and **e**) STZ-mice vehicle treated, and (**c** and **f**) STZ-mice given MLN-4760. (**a**–c) Low magnification micrographs depicting relative atrophy of medulla and widening of the cortex in STZ vehicle and (**c**) STZ MLN-4760-treated mice. Atrophy of the medulla and its tubules is most notable in STZ MLN-4760 treated mice. (**d**–**f**) High magnification micrographs showing hypertrophy of the cortex and its tubules in both STZ groups. Enlargement of tubules seems to be similar in both groups, but tubules with enlarged nuclei (red arrowheads) were readily seen in the STZ MLN-4760 group, suggesting accentuated hypertrophic response in this group.

collagen I mRNA was increased in kidney cortex from the vehicle-treated STZ mice as compared to mice from non-diabetic control group (16.42 ± 4.72 vs 1.04 ± 0.14 respectively, $P = 0.010$). MLN-4760 treatment had no significant effect on collagen I mRNA expression as compared to STZ-vehicle treated mice (13.01 ± 2.15 vs 16.42 ± 4.72 respectively, $P = 0.52$).

Electron microscopy

Ultrastructural analysis of glomeruli from STZ-treated mice showed increased mesangial matrix as compared to non-diabetic control mice, and MLN-4760 administration to STZ-treated mice was associated with a further increase in mesangial matrix as compared to STZ mice treated with vehicle (data not shown). Ultrastructural evaluation, in both MLN-4760 and vehicle-treated STZ-mice, revealed focal effacement of the foot processes, especially in the inter-capillary region with aggregation of the intracellular actin filaments (Figure 5).

In a quantitative analysis, we did not find significant differences in podocyte number between STZ mice treated with vehicle and MLN-4760 as compared to controls (open-slit pore density: control 932 ± 49/mm, STZ + vehicle 1066 ± 45/mm, and STZ + MLN-4760 1062 ± 56/mm. The number of slit diaphragms discerned by tight pore density was also not significantly different between the three groups: control 241 ± 15/mm, STZ 272 ± 17/mm, and STZ + MLN-4760 279 ± 20/mm.

Renal ACE expression

Glomerular ACE staining was increased in STZ-treated mice as compared to non-diabetic counterparts (Figure 6b and a, respectively). In STZ mice receiving MLN-4760, the number of glomeruli with strong ACE staining was increased as compared to STZ mice treated with vehicle ($65.4\% \pm 6.2$ vs $40.4\% \pm 4.9$, respectively, $P < 0.05$; Figure 6, upper panel). In renal vessels, ACE expression was also increased in the intima of STZ group as compared to non-diabetic control group (Figure 6, lower panel). In MLN-4760-treated STZ mice, the number of vessels with strong ACE protein staining was further increased as compared to STZ mice treated with vehicle ($61.3\% \pm 6.2$ vs $36.6\% \pm 6.9$, respectively, $P < 0.05$; Figure 6).

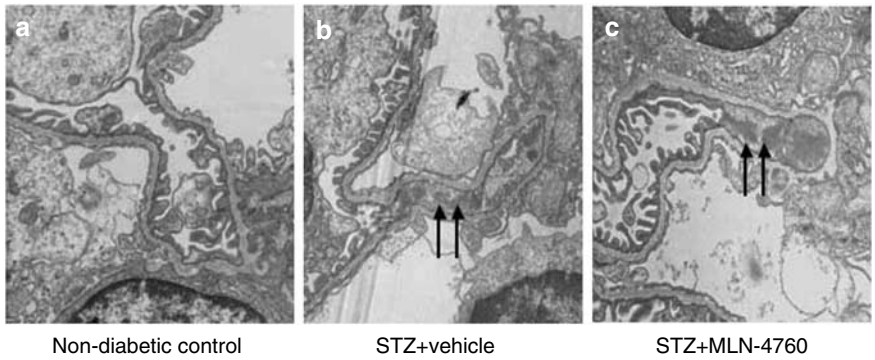

Figure 5 | Electron microscopy of glomeruli from (**a**) non-diabetic control mice, (**b**) STZ-treated mice given vehicle, (**c**) and STZ-treated mice given MLN-4760: (arrows, **b**) STZ-treated mice given vehicle and (arrows, **c**) STZ-treated mice given MLN-4760 show focal effacement of the foot processes especially in the intercapillary region with aggregation of the intracellular actin filaments as compared to non-diabetic controls (original magnification $\times 9500$).

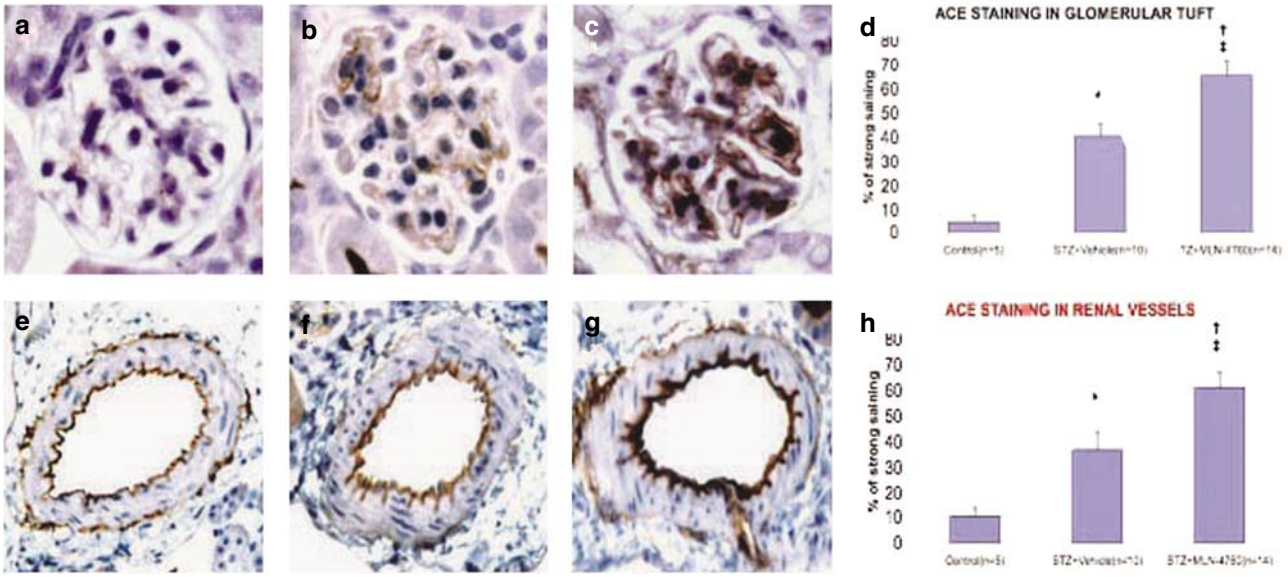

Figure 6 | Immunohistochemistry of ACE in kidney sections from (**a** and **e**) non-diabetic controls, (**b** and **f**) STZ-treated mice given vehicle, and (**c**, **g**) STZ-treated mice given MLN-4760 showing an example of glomerular and vascular ACE staining. In STZ-treated mice, ACE staining within (**b**) glomerular tuft and (**f**) vascular vessels was more intense than in (**a** and **e**, respectively) non-diabetic controls. In STZ-treated mice receiving MLN-4760, ACE staining within the (**c**) glomerular tuft and (**g**) vascular vessels was more intense than in (**b** and **f**, respectively) STZ-treated mice given vehicle. Semiquantitative analysis of (**d** and **h**) ACE immunohistochemistry (see Materials and Methods). Strong ACE staining was markedly increased within glomerular tuft and renal vessels from STZ-treated mice given vehicle in comparison with (**d** and **h**, respectively) non-diabetic control mice. After MLN-4760 administration, strong ACE staining was further increased in comparison with (**d** and **h**) STZ-treated mice given vehicle. Data are mean $\pm$ s.e. $^{*}P<0.05$ STZ + vehicle vs non-diabetic control mice. $^{\dagger}P<0.05$ STZ + MLN-4760 vs non-diabetic control mice. $^{\ddagger}P<0.05$ STZ + MLN-4760 vs STZ + vehicle.

Since both glomerular and renal vascular ACE staining showed directionally similar changes, we examined the correlation of staining intensities between these two structures. A strong positive correlation in ACE staining intensity was found between glomeruli and vessels from the same sections ($r=0.91$, $P<0.001$).

By immunohistochemistry, tubular ACE staining appeared less intense in STZ-treated mice and was further decreased by MLN-4760 administration (Figure 7a–c). The differences, however, could not be reliably quantified owing to the strong intensity of ACE staining at the tubular level.

Renal cortical ACE was therefore quantified by mRNA and enzymatic activity levels. ACE mRNA was decreased in renal cortex from the STZ mice treated with vehicle as compared to non-diabetic controls (0.51 ± 0.07 vs 1.01 ± 0.08, respectively, $P<0.001$), and MLN-4760 decreased ACE mRNA levels even further (0.27 ± 0.03, $P<0.05$; Figure 7d). ACE enzymatic activity was decreased in renal cortex from the STZ mice

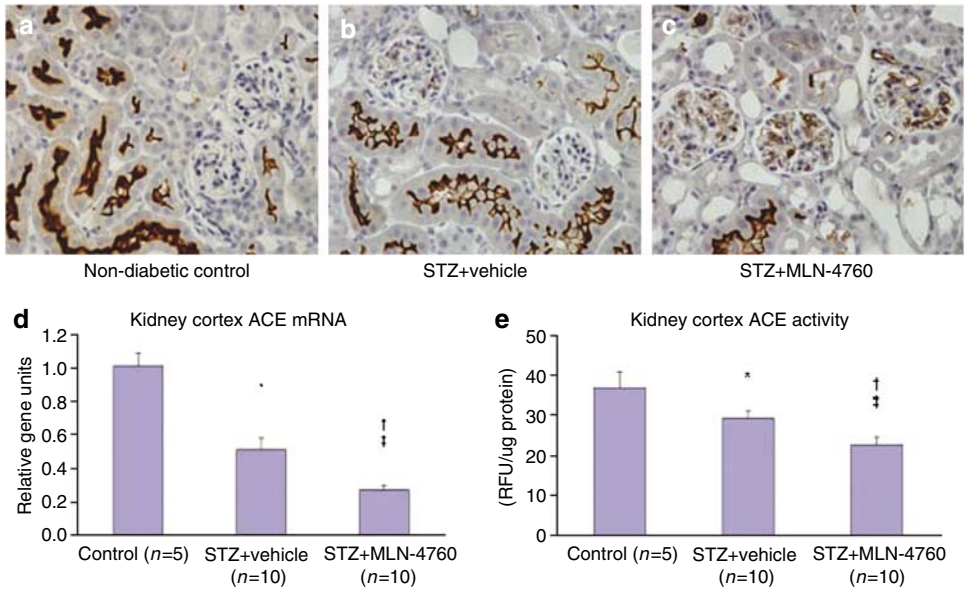

Figure 7 | Upper panel: Immunohistochemistry of ACE in kidney sections from (**a**) non-diabetic mice, (**b**) STZ-treated mice given vehicle, and (**c**) STZ-treated mice given MLN-4760 showing an example of proximal tubular ACE staining. In (**b**) STZ-treated mice, ACE staining within proximal tubules was less intense than in (**a**) non-diabetic controls. In (**c**) STZ-treated mice receiving MLN-4760, ACE staining within the proximal tubules was less intense than in (**b**) STZ-treated mice given vehicle. These findings, however, could not be quantified because of the strong staining at the tubular level in the three groups. Lower panel: (**d**) ACE mRNA and (**e**) ACE enzymatic activity in kidney cortex preparations (largely representing renal cortical tubules) from non-diabetic control, STZ-treated mice given vehicle, and STZ-treated mice receiving MLN-4760. The pattern of ACE expression in renal tubules is the reverse than that observed in glomeruli and renal vessels (Figure 6). Control: non-diabetic control mice; STZ + vehicle: STZ-treated mice given vehicle; STZ + MLN-4760: STZ-treated mice given MLN-4760. Data are mean ± s.e. $^{*}P < 0.05$ STZ + vehicle vs non-diabetic control mice. $^{\dagger}P < 0.05$ STZ + MLN-4760 vs non-diabetic control mice. $^{\ddagger}P < 0.05$ STZ + MLN-4760 vs STZ + vehicle.

treated with vehicle as compared to non-diabetic controls, and MLN-4760 decreased ACE enzymatic activity even further (Figure 7e).

DISCUSSION

This study shows that chronic inhibition of ACE2 using a specific pharmacological inhibitor, MLN-4760, worsens kidney histological lesions in the STZ mouse model of diabetes. Furthermore, MLN-4760 administration was associated with enhanced expression of ACE in both glomeruli and vasculature, suggesting that augmentation of this enzyme may play a role in the observed glomerular lesions following ACE2 inhibition. A dual mechanism of RAS activation at the glomerular level and in renal vasculature may occur during chronic ACE2 inhibition: decreased degradation of Ang II which would result in Ang II accumulation, and increased ACE expression which would result in enhanced formation of Ang II. In addition, decreased degradation of Ang II is apt to result in reduced formation of Ang 1-7, a hormone that is increasingly recognized as antiproliferative.[17–19]

A recent study in an ACE2 knockout showed the development of glomerular lesions.[8] The renal lesions occurred in male, but not female mice, and this was a late event, as it was not seen until animals were almost 1-year old.[8] In our study, by contrast, the administration of an ACE2 inhibitor for only 4 weeks to younger mice pre-treated with STZ resulted in worsening of albuminuria and glomerular histological lesions, namely mesangial matrix expansion. Of note, these findings were seen in female mice. Thus, in the setting of hyperglycemia, ACE2 inhibition appears to worsen glomerular injury. Tubular changes associated with MLN-4760 administration included tubular hypertrophy in cortical tubules. Consistent with cortical hypertrophy, the kidney/body weight ratio was also increased. The known hypertrophic effects of Ang II on proximal tubular cells[20,21] could explain these findings. After ACE2 inhibition, Ang II should increase, whereas Ang 1-7 should decrease. There is emerging evidence showing that Ang 1-7 may attenuate the hypertrophy caused by Ang II.[22,23] In contrast to these findings in the cortical areas, renal medulla and papilla were clearly atrophic in mice treated with MLN-4760 (Figure 4). It should be noted that in an ACE knockout, marked medullary and papillary atrophy are prominent findings.[24] In our study, the observed decrease in ACE tubular activity may also be the mechanism involved in the atrophic tubular lesions seen in the medulla and papilla.

MLN-4760 resulted in a significant increase in albumin excretion, but the responses were variable as it is often the case in diabetes-induced renal injury (Figure 1). We did not measure blood pressure in this study, but we have data in diabetic *db/db* mice and *db/m* controls, given this compound for a longer period of time of 16 weeks without significant effect on blood pressure (Ye *et al.*, unpublished 2006). In our study, there was no significant difference in plasma Ang II

levels in STZ animals treated with MLN-4760 and those treated with vehicle. This is an agreement with studies in ACE2 knockout where the levels of plasma Ang II were not significantly different under baseline conditions.[10] In this study, Ang II levels increased only after Ang II infusion.[10] We did not measure kidney Ang peptides in this study, as we think that the results would not be easy to interpret unless if performed separately in renal tubules and glomeruli. The isolation of tubules and glomeruli for separated measurements would be needed to examine properly the levels of Ang peptides.

Our studies using a pharmacological probe to inhibit ACE2 enzyme have advantages and disadvantages as compared to ACE2 knockout in terms of dissecting the role of this enzyme in kidney disease. Since the inhibitor used, MLN-4760, was given to adult animals, the potential effects of ACE2 ablation on kidney development, in which the RAS plays an important role, were avoided.[25] Other potential advantage is that pharmacological ACE2 inhibition does not produce complete enzymatic inhibition, a situation that resembles human disease more closely, and thereby allows for the assessment of the relative importance of ACE2. In the present study, the *in vivo* administration of MLN-4760 for 4 weeks resulted in marked inhibition of ACE2 activity in renal cortex. The specificity of this compound for ACE2 was further demonstrated using mouse recombinant ACE2 (Figure 2a), and by showing that MLN-4760 has no effect on ACE activity in isolated glomeruli or renal cortex (Figure 2b and c).

A major finding of our study is that glomerular and vascular expression of ACE was increased after chronic ACE2 inhibition using MLN-4760 administration (Figure 4). In this respect, it is important to note that a modest genetic increase in ACE levels in mice with three copies of the ACE gene resulted in an increase in albuminuria, probably as a result of RAS overactivity, when mice were made diabetic by STZ.[26] This suggests that a high constitutive level of ACE is important for the development of glomerular damage, at least in the setting of diabetes. ACE and ACE2 work in concert to regulate the level of angiotensin peptides.[27] A combination of high ACE and low ACE2 is apt to increase Ang II formation, while decreasing Ang II degradation.[7] Moreover, ACE2 inhibition would decrease Ang 1-7 formation, a peptide that has vasodilatory and antiproliferative actions.[17–19,22] We assume that the increased expression of ACE in the glomerulus reflects an augmentation of ACE in glomerular endothelial cells[7] and in the endothelium of the renal vasculature. We cannot rule out, however, the possibility that an increase of glomerular ACE also involves mesangial cells where this enzyme is also present.[28,29]

It is possible that endothelial ACE overexpression, after ACE2 inhibition, is the result of Ang II overactivity. Since Ang II upregulates gene expression and activity of ACE,[30] we surmise that Ang II overactivity may be a plausible explanation for our findings of increased glomerular and vascular ACE expression. It should be noted, however, that this effect of Ang II is tissue-specific[31] and that other studies showed no effect of Ang II on ACE secretion, whereas another study showed that chronic Ang II infusion had a weak inhibitory effect of ACE gene expression in the lung, testis, or brain.[31] Other factors that had been shown to upregulate endothelial ACE include aldosterone and vascular endothelial growth factor.[32,33] The latter seems a reasonable candidate, because it has been found upregulated in models of diabetic kidney disease and also after Ang II administration.[34,35]

Our study also confirms that there is a dichotomy between glomerular ACE and tubular ACE expression.[6,7,15] Specifically, in mice made diabetic by STZ, glomerular and vascular ACE was increased, whereas in renal cortex, a preparation that largely contains renal tubules, ACE was decreased both at the level of mRNA and enzymatic activity when compared to non-diabetic controls. Of note, similar results in terms of reduced renal cortex ACE enzymatic activity were found in STZ-treated rats by Anderson *et al.*,[36,37] and more recently by us in the *db/db* model of type 2 diabetes.[7,15] Interestingly, we now find that the administration of a specific ACE2 inhibitor decreases tubular ACE activity while increasing glomerular ACE expression, thereby replicating and exaggerating the pattern of altered ACE expression seen in diabetic kidneys. We think that the findings in the glomeruli and renal vasculature are more relevant to the pathology of diabetic kidney disease.

In conclusion, pharmacological ACE2 inhibition in STZ mice increases albuminuria and results in worsening of renal histological lesions, namely glomerular mesangial matrix expansion. ACE2 inhibition is associated with increased ACE expression in glomeruli and renal vessels. We postulate that glomerular and vascular injury associated with ACE2 inhibition is modulated, in part, by enhanced ACE expression leading to increased Ang II formation. This is apt to amplify the renal injury primarily caused by ACE2 inhibition, which leads to impaired Ang II degradation, and decreased Ang 1-7 formation.

MATERIALS AND METHODS

Animal models

All studies were conducted with the review and approval of the Institutional Animal Care and Use Committee. STZ-treated mice were used as a model of type 1 diabetes. Diabetes was induced in female C57BL/6J mice by two intraperitoneal injections of STZ (Sigma-Aldrich, St Louis, MO, USA), at a dose of 150 μg/g body weight in 50 μl of sterile 0.05 M sodium citrate (pH 4.5). The non-diabetic control group received an equal volume of vehicle, sodium citrate. Mice did not receive insulin and at 2 weeks after diabetes induction, STZ-treated mice were divided into two groups. The first group received a specific ACE2 inhibitor, MLN-4760 (kind gift from Millennium Pharmaceuticals, Cambridge, MA, USA) that was injected subcutaneously (40 mg/kg/BW, every other day) (STZ + MLN-4760). The untreated STZ group received equal volumes of sterile phosphate-buffered saline as a vehicle (STZ + vehicle). Mice were killed after 4 weeks of ACE2 inhibitor treatment at 19 weeks of age, and the last MLN-4760 dose was given about 24 h

before killing. Animal characteristics at killing are summarized in Table 1.

Blood was obtained from the tail vein and glycemia was assessed using One Touch Ultra Glucometer (LifeScan, Mountain View, CA, USA). Spot urine samples were collected before killing the mice. Urine albumin and urine creatinine were determined using Albuwell M and Creatinine Companion kit, respectively, from Exocell (Philadelphia, PA, USA) according to the manufacturer's instructions. Results are expressed as albumin/creatinine ratio (μg/mg).

Tissue preparation and morphological studies

Pentobarbital sodium was administered intraperitoneally, and kidneys were perfused with ice-cold PBS to flush out blood. Kidneys were quickly removed and weighed for morphological analysis in all experimental groups. Renal mass index was determined as the ratio of the weight of both kidneys per body weight. For pathohistological evaluation, kidneys were cut longitudinally and fixed with 10% buffered formalin phosphate (Fisher Scientific, Pittsburg, PA, USA) for overnight. Sections were stained with hematoxylin and eosin and periodic acid-Schiff.

Glomerular hypertrophy was quantified by measuring the glomerular tuft cross-sectional area with a computer image analysis system (Image J, NIH). Glomerular hypertrophy was assessed by measuring the tuft area from glomeruli in which the vascular pole was evident (using at least 20 glomeruli per section). This was performed to reduce the possibility of including tangentially cut glomeruli.[38] Glomerular images were digitalized using a colour video camera attached to a Nikon microscope ($\times 60$ objective magnification) After digitalization, the glomerular tuft was traced, and the areas were calculated using Image J (NIH) analysis software. Mesangial matrix expansion was evaluated by an experienced, masked renal pathologist using semiquantitative score (grades 1–4): 1 for normal or minimal, 2 for mild, 3 for moderate, and 4 for diffuse mesangial matrix expansion.[39,40] In addition, tubular lesions were assessed by the following semiquantitative score (grades 1–4): grade 1 = 1–25% lesions, grade 2 = 26–50% lesions, grade 3 = 51–75%, and grade 4 > 75% lesions.[16]

Immunohistochemistry

Slides were incubated for 1 h with a rat monoclonal ACE antibody (5C4) (kind gift of Dr Sergei Danilov) diluted at 1:2000, rabbit fibronectin antibody (Sigma-Aldrich) diluted at 1:400, or purified rabbit collagen type I antibody (Cedarlane, Canada) diluted at 1:500. Sections for ACE staining were washed with Tris-buffered saline Tween (DAKO, Carpinteria, CA, USA), incubated with biotinylated rabbit anti-rat IgG (Vector Labs, Burlington, Ontario, Canada) followed by peroxidase-labeled streptavidin (DAKO). Sections for fibronectin and collagen I staining were washed and incubated with goat anti-rabbit IgG conjugated with peroxidase-labeled polymer (DAKO). Peroxidase labeling was revealed using a liquid diaminobenzidine substrate-chromogen system (DAKO). Sections were counterstained with hematoxylin (Sigma-Aldrich) and dehydrated, mounted with Permount (Fisher) and coverslipped. Sections were examined and photographed with a Zeiss microscope. Non-immune antibody was used as control for specificity.

To assess levels of ACE expression in glomerular tuft and renal vasculature, a semiquantitative analysis of the immunoperoxidase-stained sections was performed based on a pathologist established score as follows: 1 = no staining; 2 = weak staining; 3 = strong staining, as described previously in other studies.[7,41,42] Sections were examined by three different masked observers, who assessed staining intensity of 100 glomeruli and 20 vessels from each slide. The data were expressed as percentage of glomeruli and renal vessels in strong staining category.

Fibronectin and collagen I expression in the tubulointerstitium was assessed by a semiquantitative analysis. The expression score from 0 to 3 was based on the intensity and distribution of fibronectin and collagen I, in which 0 represents no expression, 1 mild expression, 2 moderate expression, and 3 severe expression. In each section, the score was counted in 10 random fields under $\times 200$ magnification, and the score was averaged for each field.[43,44]

Electron microscopy

Kidney cortex was cut into 1-mm^3 blocks and fixed in 2.5% glutaraldehyde in 0.1 M sodium cacodylate buffer at 4°C for overnight. Tissue blocks were post-fixed with 2% osmium tetroxide in 0.1 M sodium cacodylate buffer for 1 h and dehydrated in graded ethanol. Blocks were infiltrated in epon/araldite resin, transferred into BEEM capsules with resin and polymerized at 60°C for 24 h. The 90 nm sections were stained with uranyl acetate and lead citrate, and examined using a JEOL 1220 electron microscope. Photomicrographs of the GBM were also analyzed for the density of open and 'tight' slit pores between the podocyte foot processes, according to published methods.[45] The number of each type of slit pore were counted and divided by the GBM length (mm) to arrive at the linear density.

ACE2 and ACE activity assay

Kidney cortex and glomerular samples were homogenized in a buffer consisting of (in mM) 50 4-(2-hydroxyethyl)-1-piperazineethanesulfonic acid, pH 7.4, 150 NaCl, 0.5% Triton X-100, 0.025 $ZnCl_2$, and 1.0 phenylmethylsulfonyl fluoride and then clarified by centrifugation at 10 000 *g* for 15 min. To each well, 88 μl of a diluted tissue sample (10 μg of total protein/well for kidney tissue extracts for ACE2 and 1 μg/well for ACE measurement) was added, along with 10 μl of buffer (with the respective inhibitor), and the reaction was initiated by the addition of 2 μl of the substrate (1.0 μM, final concentration). The plates were read using a fluorescence plate reader FLX800 (BIOTEK Instruments Inc., Winooski, VT, USA) at an excitation wavelength of 320 nm and an emission wavelength of 400 nm.[15]

Glomerular and kidney cortex ACE enzymatic activity was also assessed with a colorimetric method, as described previously[6] (ACE color; Fujirebio Diagnostics Inc., Malvern, PA, USA).[6,46] To establish whether MLN-4760 has an effect on ACE activity, protein lysates from kidney cortex and isolated glomeruli (obtained by a magnetic beads methods as described previously in Takemoto *et al.*[47]) were incubated with or without the addition of MLN-4760 (10^{-6} M) or captopril (10^{-6} M).

RNA isolation and reverse transcriptase/real-time polymerase chain reaction

Quantitative real-time polymerase chain reaction of kidney tissue samples was performed using the TaqMan Gold RT-PCR kit and ABI Prism 7700 (Applied Biosystems, Foster City, CA, USA) sequence-detection system. Primers and probes for ACE were designed using Primer Express software (Applied Biosystems). The forward primer, reverse primer, and probe were as follows: ACE gene: 5-CAGAAT CTACTCCACTGGCAAGGT-3, 5-TCGTGAGGAAGCCAGGATGT-3, and 5-FAM-CAACAAGACTGCCACCTGCTGGTCC-TAMRA-3. ACE2 gene: 5-GGATACCTACCCTTCTACATCAGC-3, 5-CTACCCCACA TATCACCAAGCA-3, and 5-FAM-CCA CTGGATGCCTCCCTGC

CC-TAMRA-3. Fibronectin gene: 5-AGATGTGCAAGCTGACAGAG ACGA-3, 5-TGTCTGGGTGACTTTCCTTGCTCA-3, and 5-FAM-ACAGTTGGTCACCCTGTTCTGCTTCA-TAMRA-3. Collagen I gene: 5-TGCTTTCTGCCCGGAAGA-3, 5-GGGATGCCATCTCGTCCA-3, and 5-FAM-CCAGGGTCTCCCTTGGGTCCTACATCT-TAMRA-3. As internal control served glyceraldehyde-3-phosphate dehydrogenase (G3PDH): with forward primer, 5-CAGAAGACTGTGGAT GGCCCCTC-3; reverse primer, 5-TGCACCACCAACTGCTTAG-3; and probe, 5-FAM-CAGAAGACTGTGGATGGCCCCTC-TAMRA-3. Reverse transcription was carried out for 30 min at 48°C. The samples were heated to 95°C for 10 min, and 40 cycles of a two-step polymerase chain reaction were performed (95°C for 15 s and 60°C for 60 s). The ACE, fibronectin and collagen I mRNA levels of the samples were normalized to their G3PDH contents. Experiments were carried out in triplicate for each data point.

ANG II levels in plasma

Blood samples were collected in tubes kept on ice containing ethylenediamine tetraacetic acid (25 mM), *o*-phenanthroline (0.44 mM), pepstatin A (0.12 mM), and p-hydroxymercuribenzoic acid (1 mM), and then centrifuged (3000 g). The plasma was removed and stored at −80°C until further processing. Angiotensin peptides were extracted from the plasma using reverse phase phenyl silica columns (100 mg; Amersham Biosciences, Buckinghamshire, UK) as per manufacturer's instructions. The quantity of Ang II in the extract was measured by enzyme-linked immunosorbent assay using commercially available kit (SPIBio, Montigny-le-Bretonneux, France).[48]

Statistical analyses

The data were reported as mean ± s.e. Significance was defined as $P<0.05$. For comparisons between two independent means, the non-parametric Mann–Whitney *U*-test was used. When more than two independent means were compared, Kruskall–Wallis test was performed. A Pearson's test was used for correlation between two variables. SPSS version 12.0 for Windows was used for statistical analyses.

ACKNOWLEDGMENTS

This work was supported by a grant from the American Diabetes Association (DB). Portions of this work were presented at the American Society of Nephrology Renal Week; 14–19 November 2006, San Diego, CA, USA. We thank Dr Sergei Danilov for providing ACE antibody. MJS performed this research work at Northwestern University Feinberg School of Medicine in Chicago, Illinois, USA as a part of her PhD thesis in the 'Universitat Autònoma de Barcelona', Medicine Department, Barcelona, Spain.

REFERENCES

1. Crackower MA, Sarao R, Oudit GY *et al.* Angiotensin-converting enzyme 2 is an essential regulator of heart function. *Nature* 2002; **417**: 822–828.
2. Donoghue M, Hsieh F, Baronas E *et al.* A novel angiotensin-converting enzyme-related carboxypeptidase (ACE2) converts angiotensin I to angiotensin 1-9. *Circ Res* 2000; **87**: E1–E9.
3. Tipnis SR, Hooper NM, Hyde R *et al.* A human homolog of angiotensin-converting enzyme. Cloning and functional expression as a captopril-insensitive carboxypeptidase. *J Biol Chem* 2000; **275**: 33238–33243.
4. Li N, Zimpelmann J, Cheng K *et al.* The role of angiotensin converting enzyme 2 in the generation of angiotensin 1-7 by rat proximal tubules. *Am J Physiol Renal Physiol* 2005; **288**: F353–F362.
5. Eriksson U, Danilczyk U, Penninger JM. Just the beginning: novel functions for angiotensin-converting enzymes. *Curr Biol* 2002; **12**: R745–R752.
6. Ye M, Wysocki J, Naaz P *et al.* Increased ACE 2 and decreased ACE protein in renal tubules from diabetic mice: a renoprotective combination? *Hypertension* 2004; **43**: 1120–1125.
7. Ye M, Wysocki J, William J *et al.* Glomerular localization and expression of angiotensin-converting enzyme 2 and Angiotensin-converting enzyme: implications for albuminuria in diabetes. *J Am Soc Nephrol* 2006; **17**: 3067–3075.
8. Oudit GY, Herzenberg AM, Kassiri Z *et al.* Loss of angiotensin-converting enzyme-2 leads to the late development of angiotensin II-dependent glomerulosclerosis. *Am J Pathol* 2006; **168**: 1808–1820.
9. Imai Y, Kuba K, Rao S *et al.* Angiotensin-converting enzyme 2 protects from severe acute lung failure. *Nature* 2005; **436**: 112–116.
10. Gurley SB, Allred A, Le TH *et al.* Altered blood pressure responses and normal cardiac phenotype in ACE2-null mice. *J Clin Invest* 2006; **116**: 2218–2225.
11. Taal MW, Brenner BM. Renoprotective benefits of RAS inhibition: from ACEI to angiotensin II antagonists. *Kidney Int* 2000; **57**: 1803–1817.
12. Carey RM, Siragy HM. The intrarenal renin–angiotensin system and diabetic nephropathy. *Trends Endocrinol Metab* 2003; **14**: 274–281.
13. Hollenberg NK, Raij L. Angiotensin-converting enzyme inhibition and renal protection. An assessment of implications for therapy. *Arch Intern Med* 1993; **153**: 2426–2435.
14. Tikellis C, Johnston CI, Forbes JM *et al.* Characterization of renal angiotensin-converting enzyme 2 in diabetic nephropathy. *Hypertension* 2003; **41**: 392–397.
15. Wysocki J, Ye M, Soler MJ *et al.* ACE and ACE2 activity in diabetic mice. *Diabetes* 2006; **55**: 2132–2139.
16. Turoni CM, Reynoso HA, Maranon RO *et al.* Structural changes in the renal vasculature in streptozotocin-induced diabetic rats without hypertension. *Nephron Physiol* 2005; **99**: p50–p57.
17. Brosnihan KB, Li P, Ferrario CM. Angiotensin-(1-7) dilates canine coronary arteries through kinins and nitric oxide. *Hypertension* 1996; **27**: 523–528.
18. Oliveira MA, Fortes ZB, Santos RA *et al.* Synergistic effect of angiotensin-(1-7) on bradykinin arteriolar dilation in vivo. *Peptides* 1999; **20**: 1195–1201.
19. Strawn WB, Ferrario CM, Tallant EA. Angiotensin-(1-7) reduces smooth muscle growth after vascular injury. *Hypertension* 1999; **33**: 207–211.
20. Wolf G, Mueller E, Stahl RA *et al.* Angiotensin II-induced hypertrophy of cultured murine proximal tubular cells is mediated by endogenous transforming growth factor-beta. *J Clin Invest* 1993; **92**: 1366–1372.
21. Wolf G, Neilson EG. Angiotensin II induces cellular hypertrophy in cultured murine proximal tubular cells. *Am J Physiol* 1990; **259**: F768–777.
22. Su Z, Zimpelmann J, Burns KD. Angiotensin-(1-7) inhibits angiotensin II-stimulated phosphorylation of MAP kinases in proximal tubular cells. *Kidney Int* 2006; **69**: 2212–2218.
23. Wang LJ, He JG, Ma H *et al.* Chronic administration of angiotensin-(1-7) attenuates pressure-overload left ventricular hypertrophy and fibrosis in rats. *Di Yi Jun Yi Da Xue Xue Bao* 2005; **25**: 481–487.
24. Esther Jr CR, Howard TE, Marino EM *et al.* Mice lacking angiotensin-converting enzyme have low blood pressure, renal pathology, and reduced male fertility. *Lab Invest* 1996; **74**: 953–965.
25. Sequeira Lopez ML, Gomez RA. The role of angiotensin II in kidney embryogenesis and kidney abnormalities. *Curr Opin Nephrol Hypertens* 2004; **13**: 117–122.
26. Huang W, Gallois Y, Bouby N *et al.* Genetically increased angiotensin I-converting enzyme level and renal complications in the diabetic mouse. *Proc Natl Acad Sci USA* 2001; **98**: 13330–13334.
27. Vickers C, Hales P, Kaushik V *et al.* Hydrolysis of biological peptides by human angiotensin-converting enzyme-related carboxypeptidase. *J Biol Chem* 2002; **277**: 14838–14843.
28. Singh R, Singh AK, Alavi N *et al.* Mechanism of increased angiotensin II levels in glomerular mesangial cells cultured in high glucose. *J Am Soc Nephrol* 2003; **14**: 873–880.
29. Camargo de Andrade MC, Di Marco GS, de Paulo Castro Teixeira V *et al.* Expression and localization of N-domain ANG I-converting enzymes in mesangial cells in culture from spontaneously hypertensive rats. *Am J Physiol Renal Physiol* 2006; **290**: F364–375.
30. Sadjadi J, Kramer GL, Yu CH *et al.* Angiotensin II exerts positive feedback on the intrarenal renin–angiotensin system by an angiotensin converting enzyme-dependent mechanism. *J Surg Res* 2005; **129**: 272–277.
31. Metsarinne KP, Helin KH, Saijonmaa O *et al.* Tissue-specific regulation of angiotensin-converting enzyme by angiotensin II and losartan in the rat. *Blood Press* 1996; **5**: 363–370.
32. Sugiyama T, Yoshimoto T, Tsuchiya K *et al.* Aldosterone induces angiotensin converting enzyme gene expression via a JAK2-dependent pathway in rat endothelial cells. *Endocrinology* 2005; **146**: 3900–3906.

33. Saijonmaa O, Nyman T, Kosonen R *et al.* Upregulation of angiotensin-converting enzyme by vascular endothelial growth factor. *Am J Physiol Heart Circ Physiol* 2001; **280**: H885–H891.
34. Cohen MP, Chen S, Ziyadeh FN *et al.* Evidence linking glycated albumin to altered glomerular nephrin and VEGF expression, proteinuria, and diabetic nephropathy. *Kidney Int* 2005; **68**: 1554–1561.
35. Kakizawa H, Itoh Y, Imamura S *et al.* Possible role of VEGF in the progression of kidney disease in streptozotocin (STZ)-induced diabetic rats: effects of an ACE inhibitor and an angiotensin II receptor antagonist. *Horm Metab Res* 2004; **36**: 458–464.
36. Anderson S, Jung FF, Ingelfinger JR. Renal renin–angiotensin system in diabetes: functional, immunohistochemical, and molecular biological correlations. *Am J Physiol* 1993; **265**: F477–F486.
37. Ingelfinger JR. ACE2: a new target for prevention of diabetic nephropathy? *J Am Soc Nephrol* 2006; **17**: 2957–2959.
38. Nakagawa T, Mazzali M, Kang DH *et al.* Hyperuricemia causes glomerular hypertrophy in the rat. *Am J Nephrol* 2003; **23**: 2–7.
39. Dai C, Yang J, Bastacky S *et al.* Intravenous administration of hepatocyte growth factor gene ameliorates diabetic nephropathy in mice. *J Am Soc Nephrol* 2004; **15**: 2637–2647.
40. Susztak K, Bottinger E, Novetsky A *et al.* Molecular profiling of diabetic mouse kidney reveals novel genes linked to glomerular disease. *Diabetes* 2004; **53**: 784–794.
41. Isbel NM, Nikolic-Paterson DJ, Hill PA *et al.* Local macrophage proliferation correlates with increased renal M-CSF expression in human glomerulonephritis. *Nephrol Dial Transplant* 2001; **16**: 1638–1647.
42. Metzger R, Bohle RM, Pauls K *et al.* Angiotensin-converting enzyme in non-neoplastic kidney diseases. *Kidney Int* 1999; **56**: 1442–1454.
43. Kaneto H, Morrissey J, Klahr S. Increased expression of TGF-beta 1 mRNA in the obstructed kidney of rats with unilateral ureteral ligation. *Kidney Int* 1993; **44**: 313–321.
44. Miyazaki Y, Tsuchida S, Fogo A *et al.* The renal lesions that develop in neonatal mice during angiotensin inhibition mimic obstructive nephropathy. *Kidney Int* 1999; **55**: 1683–1695.
45. Sung SH, Ziyadeh FN, Wang A *et al.* Blockade of vascular endothelial growth factor signaling ameliorates diabetic albuminuria in mice. *J Am Soc Nephrol* 2006; **17**: 3093–3104.
46. Kasahara Y, Ashihara Y. Colorimetry of angiotensin-I converting enzyme activity in serum. *Clin Chem* 1981; **27**: 1922–1925.
47. Takemoto M, Asker N, Gerhardt H *et al.* A new method for large scale isolation of kidney glomeruli from mice. *Am J Pathol* 2002; **161**: 799–805.
48. Volland H, Pradelles P, Ronco P *et al.* A solid-phase immobilized epitope immunoassay (SPIE-IA) permitting very sensitive and specific measurement of angiotensin II in plasma. *J Immunol Methods* 1999; **228**: 37–47.